PHYSICAL REVIEW A **72**, 041403(R) (2005)

Momentum imaging of doubly charged ions of Ne and Ar in the sequential ionization region

C. M. Maharjan, A. S. Alnaser, X. M. Tong, B. Ulrich, P. Ranitovic, S. Ghimire, Z. Chang, I. V. Litvinyuk, and C. L. Cocke
J. R. Macdonald Laboratory, Physics Department, Kansas State University, Manhattan, Kansas 66506-2601, USA
(Received 23 June 2005; published 12 October 2005)

We have measured with high resolution the full vector momenta of the doubly charged recoil ions produced when Ar and Ne atomic targets are ionized by intense circularly polarized few-cycle (~8 fs) laser pulses in the sequential ionization region. The momentum spectra of the ions were found to exhibit structure which is characteristic of the relative binding energies of the two electrons and the sequential nature of the emission process. We demonstrate that the measured spectra can be used to extract subcycle time information regarding the sequential release of the two electrons.

DOI: 10.1103/PhysRevA.72.041403 PACS number(s): 32.80.Rm

The double ionization of atoms by intense laser fields is well known to be characterized by two intensity regions, nonsequential and sequential, corresponding to different mechanisms for double electron release. In the former region, one electron is removed by the field and an associated process, usually rescattering [1–4], removes the second. In the latter region the two electrons are removed directly and sequentially by the field of the laser. The nonsequential region has received particularly heavy study in recent years, because of controversy over the mechanism, including several using momentum imaging of both recoil ions and electrons [5–9]. In this paper we turn our attention to the sequential region, and address the question: Can we follow the sequential release of the two electrons in real time?

The sequential removal of two electrons from a short pulse of electromagnetic radiation is well known and heavily studied in the area of double electron capture [10–12] from multielectron targets by slow-moving highly charged ions. This process can be described as the over-barrier electron release of the electrons from the target, on a time scale typically in the tens of femtoseconds region. This time scale is long enough that the electrons dynamically adjust to the time-dependent (classical) field. Once released from the target, the electrons usually end up captured into the strong potential of the projectile, resulting in electron capture. Probably the most comprehensive model for over-barrier multielectron capture is that given by Niehaus [10]. Some reviews which place this work in context and describe different but related treatments of the problem are described in Refs. [11–15].

This situation is very similar to the removal of electrons by a strong circularly polarized laser pulse in the "tunneling region" (i.e., small Keldysh parameter), and is the direct analog of sequential ionization in the electron capture process. In the laser case, however, the rise time of the pulse can be so long that the process is dominated by tunneling on the rising edge of the pulse, and the over-barrier field is not reached until the electrons are gone. When the pulse is short enough (we use 8 fs in this work), the time scale becomes short enough that the tunneling rate becomes quite large and over-barrier transitions become important.

A circularly polarized pulse offers two clocks with which to time the sequential release of the two electrons: a "second hand" based on the optical cycle (2.7 fs scale for 800 nm radiation) and a "minute hand" based on the pulse envelope [8 fs full width at half maximum (FWHM) for the pulses discussed here]. First we discuss this qualitatively in terms of over-barrier electron release for simplicity, although the quantitative calculations we present later in this work are done with the full consideration of the rates for the entire tunneling process. In circular polarization, the magnitude of the electric field rises smoothly to a maximum and descends again. The first (second) electron goes over-barrier when the field strength $E_1(E_2)$ reaches a value of $I_p^2/4Z$, where I_p is the ionization potential for producing an ion of a charge Z. In circular polarization, each electron emerges with zero initial momentum, and subsequently it will be acted on by the laser field to finally emerge with a momentum of magnitude $p_1 = E_1/\omega$ or $p_2 = E_2/\omega$ [16,17]. The direction of the final momentum is perpendicular to E, or in the direction of the vector potential A, at the time of emission. Given the time dependent profile of E, the measurement of p_1 and p_2 can be read back on the minute hand of the clock to provide the times at which the electrons are emitted. There is no way to extract similar information from the collisional case, where sequential electron removal occurs but the electrons are not released to the continuum. The ideal situation would be to read the second hand of the clock as well by measuring the angle between p_1 and p_2. For extremely short pulses (approaching single cycle) with the proper intensity, the time interval between the releases of the two electrons could be less than an optical cycle and this angle would just be $\omega\Delta t$, where Δt is the time delay between the releases. Using these pulses one may be able to read time on a sub-fs scale with a 2.7 fs period clock. Such an approach requires extremely short pulses and the vector momenta p_1 and p_2 of both electrons be measured. If the time delay between the releases of the two electrons exceeds 2.7 fs, the magnitude of the vector sum of p_1 and p_2 averages over this angle. However, as we discuss below, the spectrum of vector sums provides information on the individual magnitudes of p_1 and p_2. These values can in turn be interpreted in terms of the time difference between the release of the two electrons. The measurement of the vector sum of p_1 and p_2 is equivalent to the measurement of the recoil momentum of the doubly charged ion.

In this work we report on measurements of the momentum spectra of the doubly charged recoil ions produced in the sequential release of two electrons from Ar and Ne targets by circularly polarized few-cycle laser pulses at relatively high

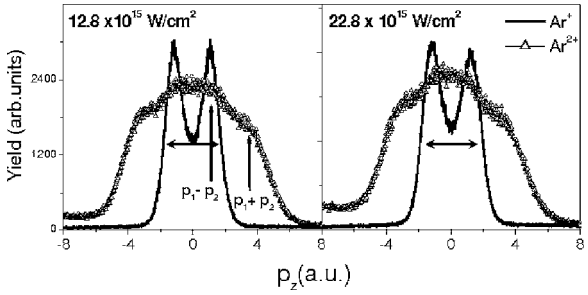

FIG. 1. Spectra of the momenta of singly and doubly ionized Ar ions projected onto the z axis (along the collection field of the spectrometer) for circularly polarized radiation at two different peak laser intensities. The horizontal arrow indicates the expected width of the single ionization peak in the over-barrier limit. The vertical arrows indicate the locations expected for two sequential over-barrier ionizations, as discussed in the text.

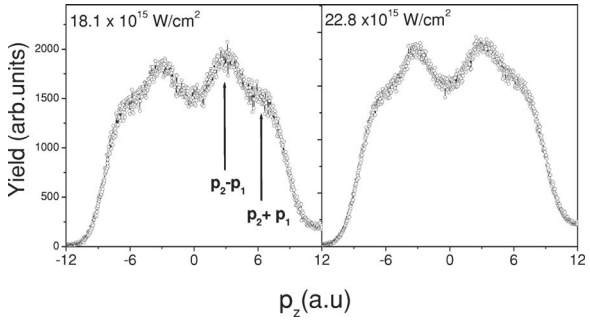

FIG. 2. Similar to Fig. 1 but for doubly charged ions only and a neon target.

intensities in the sequential ionization regime. We used a mode-locked Ti:sapphire laser with a 790 nm center wavelength amplified to pulse energies up to 2 mJ at 1 kHz repetition rate with 30 fs pulse duration. The amplified pulse was spectrally broadened in a gas-filled hollow fiber and compressed down to 8 fs by means of several bounces on chirped mirrors after the hollow fiber [18]. The pulse length and shape was measured using a FROG and found to be nearly Gaussian with pre-structure and post-structure at the few percent level. An achromatic quarter wave plate placed in the way of laser beam was used to switch from linear to circular polarization. The laser beam was focused with a 7.5-cm-focal-length on-axis spherical mirror onto a well-collimated supersonic gas jet where volume effects were minimized using piezoelectric slits. We used a standard cold-target recoil-ion momentum spectroscopy (COLTRIMS) approach [19–21], with the jet along y and the laser propagation along x, to measure and analyze the momentum distributions of the recoil-ions produced in the interactions. The ions were extracted onto a time- and position-sensitive channel plate detector by a 2 V/cm electric field in the z direction. The channel plate detector was followed by a multihit anode to measure the positions of the extracted ions. From the times-of-flight and the position the full vector momenta of these ions were obtained.

We have our best momentum resolution along the time direction, and chose to discuss first the momentum projections onto the z axis, along the extraction field and in the time direction. Figure 1 shows the p_Z spectra of Ar^+ and Ar^{2+} ions at peak intensities of 12.8 and 22.8×10^{15} W/cm^2. The singly charged ions show a shape characteristic of the projection of the expected "donut" produced in single ionization by a circularly polarized pulse. The radius of this donut can be used to deduce the value of the laser intensity [16] when one is well below the classical barrier value for single ionization, but this is not the case here. Indeed, we have taken all spectra shown here for lower intensities as well, for which the momentum spectra are intensity dependent. We chose to present the high intensity data here because we find that the shape of the spectra is no longer intensity dependent at these values, a result we attribute to being soundly in the over-barrier region. If one assumes the electron is released when the electric field reaches its over-barrier value, the radius of the donut should be given by $p_1=Ip^2/4Z\omega$. For argon and with $Z=1$, this expression yields $2p_1=2.92$ a.u. which is only slightly smaller than the observed FWHM diameter ($\sim$3.9 a.u.) of the projected single ionization spectra in Fig. 1. This result is not dependent on the actual peak intensity used, as is approximately born out by the experimental data. Note that the observed FWHM diameter is slightly larger than $2p_1$. This is to be expected, since a more quantitative examination of over-barrier ionization has shown that the ionization rate continues to rise as the field proceeds beyond the static barrier suppression value [22].

The doubly charged ions show much more complex structure, which we interpret as due to the different values of the electric field at which the two electrons are released. For high laser intensities, for which over-barrier electron release is most likely to be a correct picture, the Ar^{2+} spectra show a strong peak near zero momentum with strong shoulders on either side. We interpret this as follows: For Ar the first and second ionization potentials are 15.76 eV and 27.63 eV, respectively, corresponding to over-barrier fields of 0.084 a.u. and 0.129 a.u. (intensities of 5×10^{14} and 1.16×10^{15} W/cm^2). The corresponding values of p_1 and p_2 are 1.49 and 2.26 a.u. If the electrons were released only as the instant the field achieves these two values, not only the magnitudes of p_1 and p_2 would be unique, but the angle between them as well. However, a much more likely scenario is that each electron is released over a range of times when the field is near E_1 or E_2. If this range of times is larger than the optical cycle, the corresponding range of angles will be more than 2π. In this case one obtains recoil momenta which range between (p_1+p_2) and (p_2-p_1). Averaging over all possible angles between p_1 and p_2, as well as the absolute laboratory angle between the electric field vector and the z-axis will yield spectra which, when projected onto p_Z, lie inside and peak near p_1+p_2 and peak also at p_2-p_1. In Fig. 1 the arrows show the positions of the sum and difference of p_1 and p_2, calculated from this simple over-barrier picture. The qualitative agreement with the data is striking.

When Ne is used as a target gas (Fig. 2, for peak intensities of 18.1 and 22.8×10^{15} W/cm^2), the spectra change their character to show two strong peaks at finite values of positive and negative p_Z. with a dip near zero. We attribute the appearance of the dip to the fact that for Ne the difference

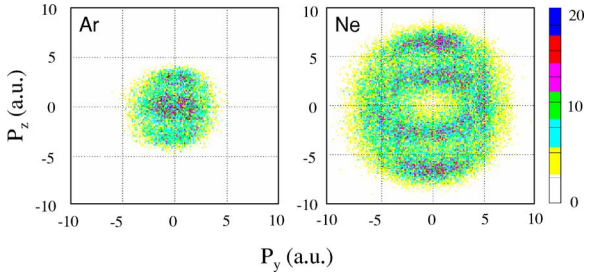

FIG. 3. (Color online) Density plots showing the projection into the y-z plane of the momenta of doubly charged argon and neon ions produced by nearly circularly polarized 8 fs pulses at a peak intensity of 22.8×10^{15} W/cm^2.

between the first and second ionization potentials (20 and 45 eV, respectively) is much greater, leading to a greater relative difference between over-barrier values of p_1 and p_2. This greater difference results in a dip for small values of (p_1-p_2) not visible in the argon case. The corresponding values for the sum and difference of p_1 and p_2 are indicated by the arrows in Fig. 2, where again qualitative agreement is obtained.

The filling of the dip near zero in the p_Z spectra is partly due to the fact that we are dealing with a p_z projection of the momentum spectra. Figure 3 shows an example of the full p_Z/p_y spectra for our experimental conditions. For the argon case there is no dip near the center of the spectrum, while for neon the dip is quite clear. This spectrum qualitatively supports the expectations discussed above. However, it also shows there is a substantial ellipticity of the radiation in our experiment. From the asymmetry of yields in the y and z directions in Fig. 3 we estimate that the ratio of A_y/A_Z (or E_Z/E_y, where A is the vector potential and E the electric field) is approximately $0.7\pm.15$. We have not yet discovered how to avoid this for such short pulses. Fortunately for this study, in the over-barrier region the ionization rate is only weakly dependent on the intensity which makes this problem less severe than it would be if we were dealing with lower intensities.

To place our interpretations on more quantitative footing, we have performed full calculations for the ionization rates to find the momentum distributions of the doubly charged Ar and Ne ions for range of laser intensities which include the saturation limits. In these calculations the field vector of circularly polarized pulse is given by

$$E(t) = E_0 e^{-2\ln 2 t^2/\tau_0^2}[\hat{e}_z \cos(\omega t+\delta) + \hat{e}_y \sin(\omega t+\delta)] \quad (1)$$

with E_0 the laser peak field, δ the carrier-envelope phase, and τ_0 pulse duration. The first and second ionization rates weighted by the survival probability can be expressed as

$$P_1(t) = W_1(t) e^{-\int_{-\infty}^{t} W_1(t')dt'}, \quad (2)$$

$$P_2(t+\Delta t) = W_2(t+\Delta t) e^{-\int_{t}^{t+\Delta t} W_2(t')dt'}, \quad (3)$$

where W_i is the ionization rate covering both tunneling and over-the-barrier ionization regions [23] for producing an ion of charge i and Δt the time delay between the two ionizations. The exponential parts are introduced to account for depletion to higher charge states by the laser field. Using the above equations, the momentum distribution of the singly and doubly charged ions can be written as

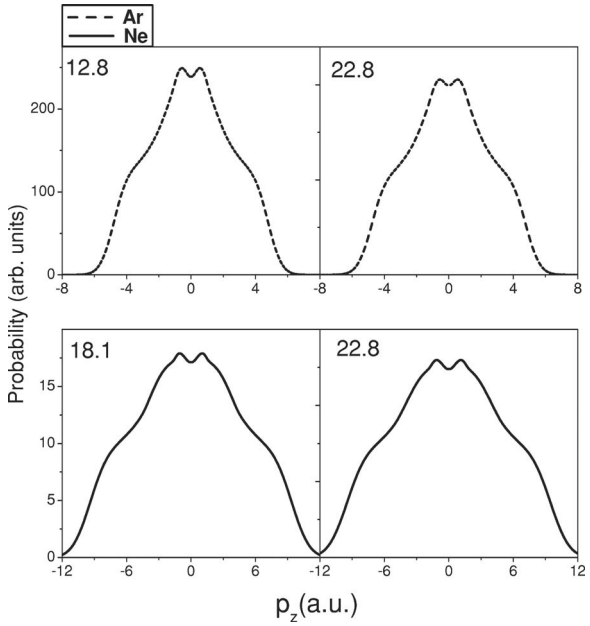

FIG. 4. Model calculations of the p_Z distributions, corresponding to the double ionization data of Figs. 1 and 2. The peak laser intensities are given in units of 10^{15} W/cm^2.

$$\frac{dP^+(p)}{dp} = \int_{-\infty}^{\infty} P_1[E(t)] e^{-\int_t^{\infty} W_2(t')dt'} \delta(p - A(t))dt,$$

$$\frac{dP^{2+}(p)}{dp} = \int_{-\infty}^{\infty}\int_{0}^{\infty} P_1(E(t)) P_2(E(t+\Delta t)) e^{-\int_{t+\Delta t}^{\infty} W_3(t')dt'} \times \delta(p - A(t) - A(t+\Delta t))dt d\Delta t \quad (4)$$

with $A(t)=\int_t^{\infty} E(t)dt$ the vector potential. Here the implicit dependence of P_1 and P_2 on time is shown through their explicit dependence on the electric field.

In order to compare with the experimental results we averaged over all possible carrier-envelope phases and included the laser pulse spatial distribution as well as depletion of singly and doubly charged ions during the pulse. Figure 4 shows the predicted momentum distributions for the Ar^{2+} and Ne^{2+} ions obtained by the above formulation. The simulated spectra are in very good agreement with the experimental results and lead to values of p_1 and p_2 that are very consistent with those predicted by the simple over-barrier model. The calculations do not show as strong a dip near $p_Z=0$ for Ne as do the data. This difference between the experiment and simulations may be due to the slight ellipticity of the light used in the experiment as well as uncertainties in the pulse shape and duration.

If one were able to perform the independent measurement of the momenta p_1 and p_2, which could be interpreted as the second hand of a clock as discussed earlier, would one expect to see an effect? We can use the present data to examine

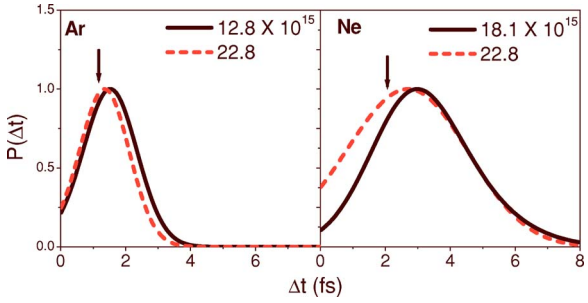

FIG. 5. (Color online) Model calculations of the distribution of time delays between the emission of the first and second electrons. The vertical arrows indicate the expected locations in the simple over-barrier picture.

this question by extracting from the present model the expected time difference between the emission times of the two electrons. If one assumes a Gaussian pulse shape with FWHM τ, the sequential emission of two electrons at field strengths E_1 and E_2 will occur with a time separation given by $\Delta t = 0.85\tau\{[\ln(E_0/E_1)]^{1/2} - [\ln(E_0/E_2)]^{1/2}\}$, where E_0 is the peak laser intensity. The resulting value for Δt is only rather weakly dependent on E_0. For a peak intensity of 22.8×10^{15} W/cm^2 the resulting time difference for argon is 1.1 fs; for neon, 2 fs.

Using the model calculation we can do better and actually calculate the time dependence of the ionization rate during the pulse. In terms of the time delay, Δt, the probability of producing a doubly charged ion can be written as

$$\frac{dP^{2+}(\Delta t)}{d\Delta t} = \int_{-\infty}^{\infty} P_1(E(t)) P_2[E(t+\Delta t)) e^{-\int_{t+\Delta t}^{\infty} W_3(t')dt'} dt. \tag{5}$$

Figure 5 shows the probability distribution for producing Ar^{2+} and Ne^{2+} ions as a function of the time delay between first and second ionizations. The peaks in this figure are remarkably close to the over-barrier values. As shown in the figure, at these laser intensities the probability of releasing two electrons from an Ar target in the same optical cycle is quite large. The delay times are substantially longer than those expected from the simple over-barrier picture, as might be expected since it is known that the ionization rate continues to rise after the field crosses the static over-barrier field strength.

In summary, we have presented recoil ion momentum spectra for doubly charged argon and neon ions produced by very short (8 fs FWHM) pulses of (nearly) circularly polarized radiation. The spectra show structure which can be interpreted qualitatively in terms of two successive over-barrier ionizations. This interpretation is supported by a detailed model calculation of the whole time-dependent process. We explore the implications of this simple picture, and the quantitative model, for the time sequence for the emission of the two electrons. We find that the time delay between emission of the two electrons can easily be less than a single optical cycle for the case of argon. This conclusion is based on reading the "minute hand" clock provided by the known time dependence of the pulse envelope. This experiment is a predecessor to one in which a "second hand" of the rotating electric field vector could be used to read this time difference with a precision much less than the optical period. This clock could be read by measuring the individual vector momenta of the two electrons and deducing the angle between the vectors. Such an experiment is most meaningful if the two ionizations are separated by less than a single optical cycle, which seems likely to occur for argon but not for neon. It would be particularly interesting if this clock were applied to time other events occurring in the system such as the fragmentation of a light molecule.

ACKNOWLEDGMENTS

This work was supported by the Chemical Sciences, Geosciences and Biosciences Division, Office of Basic Energy Sciences, Office of Science, U. S. Department of Energy. We acknowledge stimulating conversations with P. Corkum and R. Dörner in the early stages of this work.

[1] P. B. Corkum, Phys. Rev. Lett. **71**, 1994 (1993).
[2] G. L. Yudin and I. Y. Ivanov, Phys. Rev. A **63**, 033404 (2001).
[3] H. Niikura *et al.*, Nature **417**, 917 (2002).
[4] X. M. Tong *et al.*, Phys. Rev. Lett. **91**, 233203 (2003).
[5] Th. Weber *et al.*, Phys. Rev. Lett. **84**, 443 (2000).
[6] R. Moshammer *et al.*, Phys. Rev. Lett. **91**, 113002 (2003).
[7] A. S. Alnaser *et al.*, Phys. Rev. Lett. **91**, 163002 (2003).
[8] A. Rudenko *et al.*, Phys. Rev. Lett. **93**, 253001 (2004).
[9] M. Weckenbrock *et al.*, Phys. Rev. Lett. **92**, 213002 (2004).
[10] A. Niehaus, J. Phys. B **19**, 2925 (1986).
[11] E. Salzborn and A. Müller, in *Physics of Electronic and Atomic Collisions*, edited by Oda and Takayanagi (North-Holland, Amsterdam, 1988), p. 407.
[12] E. K. Janev and L. P. Presnyakov, Phys. Rep. **70**, 1 (1981).
[13] M. Barat and P. Roncin, J. Phys. B **25**, 2205 (1992).
[14] C. L. Cocke and R. E. Olson, Phys. Rep. **205**, 153 (1991).
[15] *Review of Fundamental Processes and Applications of Atoms and Ions*, edited by C. D. Lin (World Scientific, Singapore, 1993), Chpts. 3 and 6, p. 111, and p. 239.
[16] A. S. Alnaser *et al.*, Phys. Rev. A **70**, 023413 (2004).
[17] P. B. Corkum *et al.*, Phys. Rev. Lett. **62**, 1259 (1989).
[18] M. Nisoli *et al.*, Opt. Lett. **22**, 522 (1997).
[19] R. Dörner *et al.*, Phys. Rep. **330**, 95 (2000).
[20] J. Ulrich *et al.*, Rep. Prog. Phys. **66**, 1463 (2003).
[21] S. Voss *et al.*, J. Phys. B **37**, 4239 (2004).
[22] A. Scrinzi *et al.*, Phys. Rev. Lett. **83**, 706 (1999).
[23] X. M. Tong and C. D. Lin, J. Phys. B **38**, 2593 (2005).